



Revalorization of chromium-tanned leather shavings into carbon materials and re-tanning solution

Javier A. Arcibar-Orozco¹ · Adriana Saldaña-Robles² · Rene Rangel-Méndez³ · Lilja Nielsen⁴ · Hazael Baltazar-Campos¹ · Estefany A. Garduño-Cruces⁵ · Blanca Valeria Hernandez-López¹ · Felipe Caballero-Briones⁶

Received: 24 November 2022 / Revised: 9 February 2023 / Accepted: 27 February 2023 / Published online: 9 March 2023
© The Author(s), under exclusive licence to Springer-Verlag GmbH Germany, part of Springer Nature 2023

Abstract

Tanned leather is a product of high intrinsic value and a sign of luxury. Chromium-tanned leather shavings are abundantly produced wastes which contain chromium that could be revalorized. The present research proposes the use of alkaline hydrolysis, aided by an inorganic anion, to promote the hydrolysis of the Cr–O bond. De-chromed solids were employed to synthesize carbon material, which subsequently was applied for dye removal from aqueous solution, while the chromium-rich solution was used as a re-tanning agent. The results demonstrated that it is possible to develop a method of chromium-protein separation, with a minimum degree of hydrolyzation. When an activating agent was employed, the prepared carbon had a surface area of 585 m²/g, with trace levels of chromium (<0.1%), present mainly as Cr₂O₃ particles. The materials displayed an adsorption capacity of up to 47.60 mg/g and 27.58 mg/g for methylene blue and Congo red respectively. The chromium-rich solution contained proteins and amino acids that aid in its employment as a re-tanning agent. Leather that was re-tanned with this solution had a similar tear strength and a superior and tensile strength (38%), superior elongation at break (10%), and improved elongation at break (47%) than traditional Cr33-tanned leather. The present study represents a major step in the development of cleaner production of leather.

Keywords CTLS · Carbons · Adsorption · Dye removal · Re-tanning · Waste revalorization

✉ Javier A. Arcibar-Orozco
Javier.arcibar@gmail.com

- ¹ Department of Research and Technological Solutions, CIATEC A.C. Centro de Innovación Aplicada en Tecnologías Competitivas, Omega 201, Industrial Delta, 37545 León, GTO, Mexico
- ² Department of Agricultural Mechanical Engineering, Universidad de Guanajuato, 36500 Irapuato, GTO, Mexico
- ³ Institute for Scientific and Technological Research of San Luis Potosi, 78545 San Luis Potosi, San Luis Potosí, México
- ⁴ Department of Biological Sciences, Kingsborough Community College, 2001 Oriental Blvd., Brooklyn, NY 11235, USA
- ⁵ Unidad Profesional Interdisciplinaria de Ingeniería Campus Guanajuato, del Instituto Politécnico Nacional Campus Guanajuato, Av. Mineral de Valenciana 200, 36275 Silao, Guanajuato, México
- ⁶ Instituto Politécnico Nacional, Materiales Y Tecnologías Para Energía, Salud y Medio Ambiente (GESMAT), CICATA Altamira, Km 14.5 Carretera Tampico-Puerto Industrial Altamira, 89600 Altamira, México

1 Introduction

In the history of leather production, the processing step has long been associated with hazardous pollution and compromised health. Nonetheless, its production is of high demand due to its unique features. During its processing, a large amount of solid wastes and wastewater are generated; it has been estimated that for every ton of raw hide/skin processed, 800 kg of solid and up to 50 m³ of liquid wastes are produced [1]. Among such wastes, one of the most critical, due to the amount produced and the hazard that it presents, are the Chromium (or Chrome)–Tanned Leather Shavings (CTLS). These wastes are sometimes dumped into landfills without further treatment, representing a serious threat to the environment [1]. Furthermore, studies have postulated that when certain conditions are met, Cr can be oxidized and lixiviated from leather wastes and goods, affecting human health [2].

Nonetheless, leather production is still a growing demand [3]. In order to achieve sustainable leather

production, it is necessary to develop a feasible process(es) for the prevention, treatment, and revalorization of CTLS. In the literature, there are some examples of physicochemical processes aimed at upcycling CTLS including fertilizers [2], anaerobic digestion to obtain energy [4], chromium recovery [5], gelatin obtention for use as an adsorbent [6], and ultimately for the production of new useful materials such as coagulants [7], shielding materials [8], catalysts, oxidants, and adsorbents [9, 10], among others. Some methodologies have focused on processing CTLS for recycling in the tanning facility either as re-tanning agents [11] or as recycled leather [12].

CTLS have a chemical composition similar to that of tanned leather, consisting of α -collagen, in which carboxylic groups are stabilized by chromium(III) complexes, by means of covalent coordination bonds. Therefore, CTLS are rich in both collagen and chromium. The former is a valuable material with applications in various fields, such as cosmetics, feedstock, and medicine, whereas the chromium can be recycled within the tanning facility into a tanning/re-tanning material or for other applications such as glass making and catalyst materials [1]. The key for the processing of such waste lies in the hydrolytic separation of the collagen and chromium, which can be carried out by means of acidic, basic, thermal, and/or enzymatic treatments. In the literature, there are numerous examples of these methods demonstrating that it is possible to partially, as well as completely, hydrolyze such wastes [13–16]. However, a proper physicochemical treatment must, in principle, only hydrolyze the Cr–O–C bond, rather than all the protein, thereby providing for easier separation and processing. A simple method consists of NaOH with an organic salt complexing agent (i.e., tartrate anion), which assists in keeping chromium soluble and protects hydrolyzed bonds from further degradation [13, 17].

Once separated, non-hydrolyzed protein can be processed to obtain several goods, including precursor carbon materials such as biochar and activated carbon [18], while the liquid solution containing chromium can be recycled in the tannery facility. In the present article, we propose a basic hydrolysis (with NaOH) aided by potassium tartrate to hydrolyze CTLS, and then a separation of the hydrolysate into (1) solid de-chromed tanned leather shavings (DTLS), that will be employed as a precursor for both biochar and activated carbon, and subsequently studied for the removal of hazardous dyes from aqueous solution, and (2) a chromium-rich liquor, that will be employed as a re-tanning agent. To the best of our knowledge, this is the first study that proposes the simultaneous valorization of CTLS as low chromium-content carbons and re-tanning liquor.

2 Materials and methods

2.1 Materials

All reagents employed, sodium hydroxide, potassium tartrate (K-tar), zinc chloride, and hydrochloric acid, were of analytical grade (purity higher than 99%), with exception of sodium formate, industrial grade, and purity of 95%. CTLS were acquired from a local tannery facility located in León City, Mexico. Before any analysis or treatment, CTLS were rinsed several times with deionized water (resistivity higher than 18 M Ω /cm), to remove any impurities. CTLS were characterized and reported elsewhere [19]. The proposed methodology for CTLS integral valorization is displayed in Fig. 1.

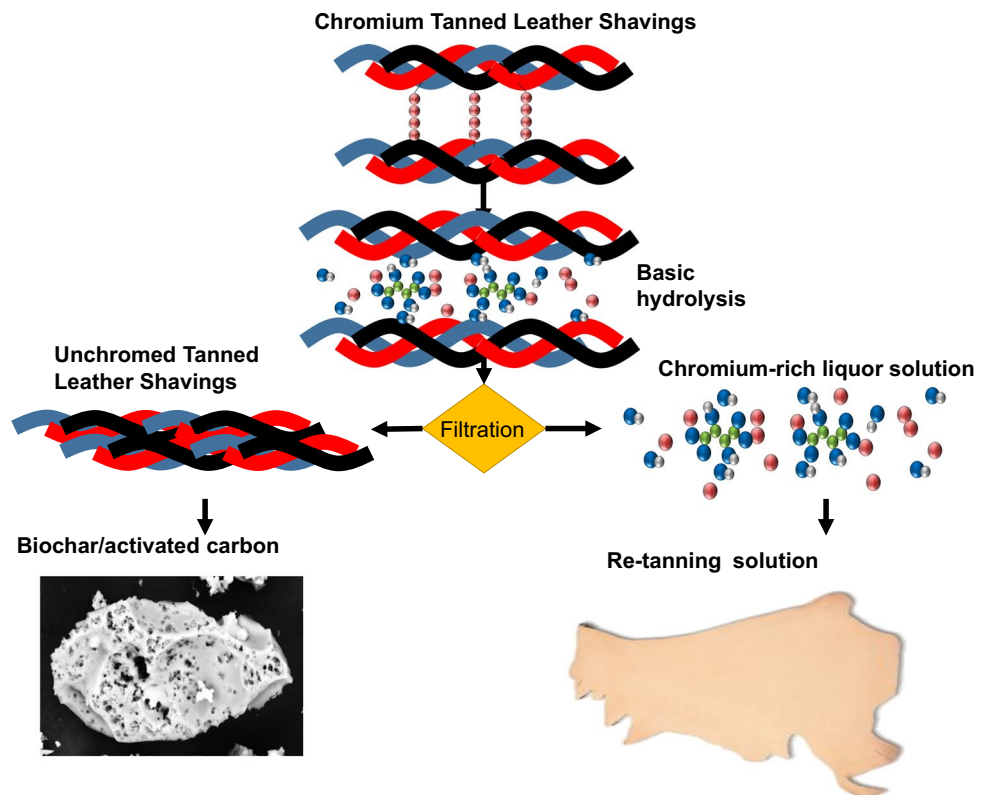
2.2 Strategy for chromium extraction; alkaline hydrolysis

The basic hydrolysis of CTLS was carried out by preparing an extracting solution consisting of NaOH and potassium tartrate (K-tar). An experimental design, described in Section 2.3, was used to define the concentrations. Five grams of dried CTLS was contacted with 50 mL of the solution for 24 h and kept under constant stirring to promote hydration. Then, 50 mL of a solution containing the proper amount of NaOH and K-tar was added. The solutions were kept under constant stirring during 24 h. After that time, 0.1 M HCl was added up to a pH of 7, in order to stop the reaction, and immediately after, the suspension was filtered (Whatman@ 45 μ m) to obtain a chromium-rich liquor solution and De-chromed Tanned Leather Shavings (DTLS) solids. DTLS were rinsed with deionized water to remove any residues from the hydrolysis solution, and then dried at 60 °C. Chromium content was determined by Atomic Absorption Spectroscopy (AAE) in an iCE 3000 (Thermo).

2.3 Experimental design and analysis

To study the effect of both NaOH and K-tar concentrations on the Cr extraction percentage and remaining mass, an experimental central composite design (CCD) 2^2 with four factorial points, four axial points, and three central points was proposed (see Table S1). The experimental design was carried out in triplicate, and the variance analysis was carried out for both response variables, namely, Cr extraction percentage and the percentage of remaining mass. The CCD in Response Surface Methodology (RSM) was employed for the single and multiple optimization response designs. The variance analysis analyzed the

Fig. 1 Proposed methodology for the processing of CTLS to yield the following products: biochar/activated carbon and re-tanning agent



significance of concentration parameters and their square interaction. The sum of squares, the mean square, and the *F*-ratio and *P*-values of the classical ANOVA analysis were calculated; significance was observed when the *P*-value was less than 0.05.

2.4 Transformation of DTLS into biochar and activated carbon

Carbon materials were obtained via pyrolysis in a tubular furnace, under a constant N_2 flow of 100 mL/min. The DTLS were heated from room temperature to 600 °C or 800 °C, at a heating rate of 10 °C/min. Biochars were obtained at 600 °C and 800 °C, named CR_600 and CR_800 respectively. Additionally, one activated carbon was obtained at 800 °C by mixing the DTLS with $ZnCl_2$ at a mass ratio of 1:1 prior to pyrolysis; the material was named CR_800Zn. Carbon materials were demineralized by contacting them with 1 L of 10% HCl and heating them to the boiling point. This procedure was repeated until no remains of Zn or Cr were detected in the demineralizing solution. After, the carbons were washed with DI up to a constant pH and finally dried at 100 °C for 12 h.

2.5 Characterization of carbon materials

Fourier transform infrared (FT-IR) spectroscopy was done in a Nicolet i50 (Thermo); the data was collected in total attenuated reflectance mode, and 32 spectra were obtained and averaged. XRD data were obtained with a Bruker D8 Advance, using $Cu K\alpha$ radiation source in the Bragg–Brentano geometry, and an analysis step of 0.02°. Scanning electron microscopy (SEM) was conducted in a Quanta microscope. The materials were crushed and mounted on a carbon fiber before analysis, and the image was obtained with an electron acceleration of 5.0 keV. XPS was obtained in a K-Alpha surface analysis system from Thermo Fisher Scientific, with an incident monochromated $Al K\alpha$ X-ray beam source (1486.6 eV). N_2 physisorption isotherms were obtained in an ASAP 2020 (Micromeritics); prior to analysis, the materials were degasified at 120 °C for 4 h. Surface area was calculated by using the Brunauer-Emmet-Teller equation (S^{BET}). Potentiometric titration was obtained by the procedure described previously [20]. The data was transformed into a proton binding curve that represents a continuous pK_a distribution, obtained by using the SAIEUS software, and according the Jagiello procedure [21]. The pH at the point

of zero charge (pHPZC) is defined as the intercept of the x -axis.

2.6 Adsorption experiments

Two dyes were selected as adsorbates: Congo red (CR) and methylene blue (MB). The procedure for obtaining the adsorption isotherms was the following: 50 ± 0.5 mg of the selected carbon material was contacted with 30 mL of a solution containing a desired concentration of dye, selected between 10 and 100 mg/L. The dye-containing solution was adjusted to a pH of 7, and then kept stirring at 25 °C for 5 days to achieve equilibrium. Daily adjustments with NaOH/HCl 0.01 M were done to ensure a constant pH. After, the experiments were centrifuged, and aliquots of 5 mL were taken. The concentration of the dye was determined by using a UV–Vis spectrometer. The wavelengths selected for the dyes' quantification were 496 nm for CR and 663 nm for MB; they were selected as the maximum adsorption wavelength in a scan of aqueous solutions containing 1 ppm of each dye separately (Figure S1). Adsorption capacities were calculated by mass balance in the batch reactor. Adsorption data were adjusted to the Langmuir (Eq. 1) and Freundlich (Eq. 2) models, and the R^2 fitting function was reported.

$$Q = \frac{Q^{max} * b * C_e}{1 + b * C_e} \quad (1)$$

$$Q = KF * C_e^{(1/n)} \quad (2)$$

where Q is the adsorption capacity at the equilibrium concentration C_e , b is the Langmuir constant, Q^{max} is the monolayer maximum adsorption capacity, KF is the Freundlich constant, and n is the heterogeneity factor of the Freundlich model.

2.7 Chromium-rich liquor characterization

In order to be characterized, the chromium in the rich liquor was separated by means of precipitation with H_2SO_4 ; a titration-precipitation curve was obtained to determine the amount of H_2SO_4 necessary to form insoluble $CrSO_4$ (Figure S2). The de-chromed liquor was separated by centrifugation and filtration with a 0.45 μ m membrane. The protein content of the liquor was estimated using the Bradford assay, with a bovine protein standard [22]. Amino acids were separated and analyzed by ion chromatography in a DIONEX ICS 5000 (Thermo), including an AminoPac PA10 column with an electrochemical detector. NaOH (250 mM) and sodium acetate (1 M) were used as eluent, at a flow of 0.25 mL/min. A gradient method was employed

to separate the following amino acids: arginine (1.3 min), lysine (3.0 min), alanine (5.9 min), threonine (6.3 min), glycine (7.0 min), valine (8.4 min), serine (9.7 min), proline (10.7 min), isoleucine (14.0 min), leucine (15.4 min), methionine (16.1 min), histidine (20.9 min), phenylamine (22.6 min), glutamate (24.2 min), aspartate (24.8 min), cysteine (26.0 min), tyrosine (29.2 min).

2.8 Application of chromium-rich liquor as a re-tanning agent

Chromium- and amino acid-rich liquor was employed as a re-tanning agent in a pilot-scale drum. A wet blue chromium-tanned cow leather served as the raw material; the characteristics of the blue leather are presented in Table S2. The formula for re-tanning is displayed in the Supplementary Information (Table S3). The leather re-tanned with chromium-rich liquor was compared to one re-tanned with commercial Cr33. Finished leather was evaluated to determine its tear strength, tensile strength, elongation at break, and tear according the ISO norms for leather [23]. For the evaluation of subjective properties such as softness, tact, filling, and color intensity, a panel of experts was asked to blind evaluate both leathers on a scale of 1 to 5.

3 Results and discussion

3.1 Selective hydrolysis of chromium compounds

The dynamic extraction experiments demonstrated that 24 h (Figure S3) was sufficient time to reach about 80% of the total chromium recovery. For that reason, the extraction experiments were conducted at 24 h.

The objective of the present work was to fracture the covalent bonds of the Cr linkage, while maintaining the structural integrity of the collagen, thus the experimental design required finding a balance between hydrolyzing Cr and protein integrity. Of course, it is virtually impossible to employ a chemical strategy to selectively hydrolyze the Cr–O–C bond (Cr bonds covalently to the carboxylic groups in collagen) without affecting the integrity of the hydrogen and peptide bonds. Our first experimental approach was to design an extraction experiment based on known hydrolytic conditions that favor Cr removal. The response variables were the % of Cr recovery and the % of degradation of CLTS degradation, calculated as the amount of mass that remained after extraction (Table 1).

As mentioned above, the objective of the present work is the comparison of a single-objective optimization with respect to a multiple-objective optimization, in order to find the most reliable technique for the two-variable optimization procedure. The results of the variance analysis for Cr

Table 1 Results of the experimental conditions employed

Concentration NaOH	Concentration K-tart	% Chromium recovery	% Remaining mass
0.05	0.75	61.4	86.9
0.15	0.75	92.4	0.0
0.05	2.25	51.5	89.2
0.15	2.25	86.7	82.7
0.03	1.5	54.0	91.1
0.17	1.5	95.1	79.2
0.1	1.5	71.8	70.0
0.1	0.44	66.6	47.8
0.1	2.56	51.5	63.5
0.03	0.25	23.3	96.8
0.08	0.25	48.4	81.2
0.03	0.75	42.7	96.2
0.05	0.5	57.1	90.6
0.08	0.75	75.1	94.0

extraction %, as well as the % of remaining mass, show that the effects of both experimental factors (NaOH and K-tar) have *P*-values of less than 0.05, which indicate that they are significantly different from zero at the 95.0% confidence level, with R^2 of 85.6 and 75.6, respectively (see Table 2). In addition, an interesting interaction occurred among the factors in source AB (A is NaOH and B is K-tar), which had a statistical significance on the % of remaining mass (*P*-value < 0.05). By diminishing the NaOH and increasing the K-tar, the % of remanent mass could be increased to a significant level. These results were analyzed through the response surface methodology (RSM), focused on the single optimization of Cr extraction %, as well as the % of remaining mass. It was found that the optimal concentrations for NaOH and K-tar to extract 95.1% of Cr were 0.17 M and 1.5 M, respectively; however, the remaining mass was decreased to 79.2%. It was found that the optimal conditions for retaining mass (nearly 98%) were achieved using

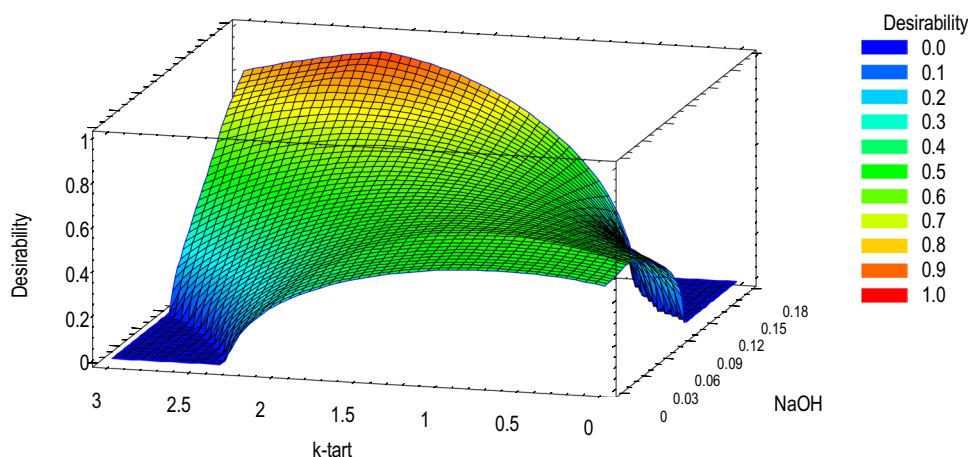
0.04 M NaOH and 1.23 M K-tar; however, this decreased the percentage of Cr extracted to 81%. It was observed that higher NaOH concentrations benefit Cr extraction, while lowering the concentration benefits the remaining mass, thus the NaOH concentration must be adjusted to meet the objectives of the study. Since it is not possible to optimize a single-objective parameter without negatively affecting a second, the present work intends to maximize the % of Cr extracted, as well as the % remaining mass, and thus a multiple response optimization is required. In the literature, the primary focus has been on maximizing the % of Cr extracted, for instance 90% of extracted Cr was obtained by employing K-tar in an alkaline medium [24], whereas 96% of Cr was extracted by optimizing the NaOH to 0.17 M. [13].

In order to simultaneously optimize the two objectives, a RSM with the multiple response optimization was employed, and the results showed that in the combination of concentrations of NaOH and K-tar of 0.17 M and 2.28 M, respectively, an optimum response of 88.61% Cr extraction and 97.4% remaining mass were obtained. The RSM in Fig. 2 shows the desirability of optimum response, as well as the behavior of desirability function, based on the factors mentioned above. It is observed that optimal results correspond to concentrations of K-tar ranging from 2.5 to 1.5 M, and a NaOH concentration ranging from 0.16 to 0.18 M. Both concentration ranges are found within the desirable region that maximizes the Cr percentage of extraction as well as the remaining mass. By comparing the results in the RSM multiple response optimization with the RSM single response optimization, it is observed that an optimal combination for the input concentrations (NaOH and K-tar) allows for maximization of both response factors. The RSM multiple response optimization is the most suitable analysis technique to study and optimize in the case of more than one objective for the input variables. In a previous work [16], RSM was employed to optimize the % of Cr extracted from solid leather, and it was found that to extract 88% of Cr required 0.375 M NaOH at 60 °C. In the present study, it was possible to obtain higher extraction

Table 2 Variance analysis for Cr extraction and remaining mass percentage

Cr extraction						Remaining mass					
Source	Sum of squares	Df	Mean square	F-ratio	P-value	Source	Sum of squares	Df	Mean square	F-ratio	P-value
A:NaOH	4863.2	1	4863.2	80.16	0.0000	A:NaOH	4547.45	1	4547.45	17.45	0.0004
B:K-tar	511.601	1	511.601	8.43	0.0082	B:K-tar	4313.48	1	4313.48	16.55	0.0005
AA	118.445	1	118.445	1.95	0.1763	AA	544.534	1	544.534	2.09	0.1624
AB	13.1252	1	13.1252	0.22	0.6464	AB	4840.08	1	4840.08	18.57	0.0003
BB	120.266	1	120.266	1.98	0.1731	BB	1036.47	1	1036.47	3.98	0.0587
Blocks	92.5363	2	46.2682	0.76	0.4784	Blocks	453.283	2	226.641	0.87	0.4330
Total error	1334.73	22	60.6697			Total error	5733.65	22	260.62		
Total (corr.)	7253.51	29				Total (corr.)	22,557.8	29			

Fig. 2 Surface response of desirability of Cr extraction/conservation of mass employed in the experimental design and analysis



percentages with the advantages of less NaOH use and room temperatures. The present work shows a similar percentage of recuperation; however, the multi-response methodology, besides clarifying the high Cr extraction, enables determination of a high percentage of remaining mass. The selected condition can be applied towards the production of activated carbon, and moreover could be accomplished with less than half the concentration of NaOH of that employed by [16]. For the reasons discussed above, the following condition was selected for UCTLS obtention and subsequent carbon materials production: NaOH concentration of 0.17 M, K-tar concentration of 1.5 M.

3.2 Production of activated carbon from de-chromed tanned leather shavings

In previous studies, activated carbon (AC) has been synthesized directly from CTLS, resulting in interesting materials capable of performing in different applications including adsorption, oxidation, and catalysis [19, 25, 26]. However, a major drawback in the application of these materials lies in the remaining presence of chromium particles, which may pose a hazard. In this work, the use of DTLs as precursor for AC production will eliminate the formation and deposition of chromium particles.

The yield of the synthesized materials, as well as the elemental composition, is provided in Table 3; note that all yields were below 22%. In principle, DTLs are composed of collagen and hydrolyzed collagen, which have decomposition temperatures around 145 and 240 °C, respectively

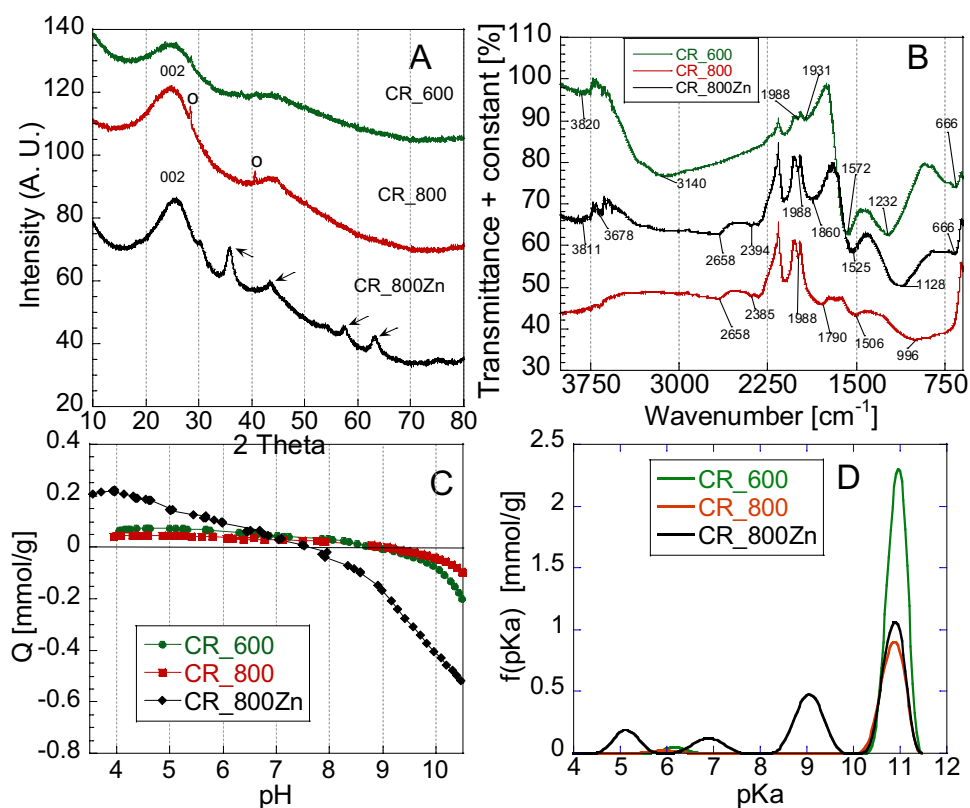
[27]. Since the hydrolysis process consists of breaking the covalent bonds of the Cr–O-matrix and the peptide bonds of the collagen structure as well, it is expected that when DTLs undergo the pyrolysis process, there is considerable gasification of the already hydrolyzed fibers, leading to a low yield. Such a yield is lower during the production of activated carbon than of biochars, which is a natural result of pore creation during dehydration with $ZnCl_2$ at high temperatures. On the other hand, all of the materials displayed a low ash content (lower than 8%), with a considerably low content of chromium, corroborating that the hydrolysis process is successful in obtaining a precursor for biochar and activated carbon of low inorganic content. When comparing this chromium content with that reported in previous studies employing CTLS directly [19], the decrease in chromium content was significant (from 0.8 to 0.09%). Indeed, the chromium content detected in the current materials is lower as compared to other studies available in the literature (i.e., 27.46–42.16% [28], 10.00–13.00% [29], 2.00% [30], 1.20–3.21% [31], and 1.30–0.63% [32]).

The general characterization of the materials is represented in Fig. 3. XRD of carbon materials (Fig. 3A) revealed the presence of widened (002) peaks related with graphite, which is a normal feature of amorphous carbons with disordered aromatic rings [33]. It is interesting to observe the presence of a crystalline (002) peak at 28.4 2 θ and (100) peak at 40.7 2 θ of graphite in the sample CR800 (denoted as 0). This indicates the coexistence of graphitic and amorphous structures (turbostratic carbon) [34], which are probably induced by the higher carbonization

Table 3 Yield and elemental content of the synthesized materials

Material	Yield [%]	Ash [%]	C [%]	N [%]	H [%]	Zn [%]	Cr [%]
CR_600	21.92	6.88	64.76	13.02	2.81	0	<0.01
CR_800	21.44	7.69	68.17	9.87	3.75	0	0.16
CR_800Z	15.76	5.54	71.06	7.93	3.92	0.06	0.09

Fig. 3 Characterization results of biochars (CR600 and CR800) and activated carbon (CR800Zn) displaying **A** XRD, **B** FT-IR, **C** surface charge distribution, and **D** pK_a distribution



temperature employed during the material's synthesis. Sample CR_800Zn displayed the typical features of amorphous microcrystalline carbons, without the crystalline feature of graphite mentioned above. This is attributed to the activating effect of ZnCl₂ that creates porosity, contributing to the microstructure of the material. The diffractogram also displayed widened peaks of CrO (JCPDS 06–0532), at about 35°, 43°, 54°, 57°, and 63° 2θ, marked with arrows [35]. It is interesting to compare samples CR_800 and CR_800Zn, since both were subjected to the same carbonization conditions, but with the presence of ZnCl₂ for activation. It is possible that the ZnCl₂ presence is promoting the formation of insoluble CrO particles on the carbon materials.

The FT-IR spectra of the materials are displayed in Fig. 3B. The materials displayed a few bands that could be related with oxygen groups. The first wide band at around 3811–3820 cm⁻¹ (absent in sample CR_800) is related with bulk OH groups; bands at 1988 cm⁻¹ could be related with C=O bands; and the bands at 1232 cm⁻¹ on CR_600 and 1128 cm⁻¹ on CR_800Zn could be attributed to C-O groups. The other bands were attributed to chemical functionalities such as aromatic rings (1505–1572 cm⁻¹), nitrogenated compounds (3678–3140 cm⁻¹), and probably Cr-O vibrations (at 666 cm⁻¹).

The results of the potentiometric titration are presented as a proton binding curve (Fig. 3C). On the non-activated biochars, there was a low surface charge (in terms of the

amount of adsorbed or released protons from the surface) that yielded a basic pH_{PZC} of about 8.8. It is well recognized that most of the acidic charge in carbons comes from surface oxygen groups; therefore, the low pH_{PZC} can be linked to the low content of oxygen surface groups. In contrast, CR_800Zn had a more acidic surface, with a pH_{PZC} of about 7.5. This is the result of the introduction of a small number of hydroxyl groups that release protons upon hydration. Indeed, the deconvolution of the proton binding curve (Fig. 3D) displays that on biochars CR_600 and CR_800, there is a lack of functionalities of low pK_a , which traditionally have been associated with carboxylic groups, and only high pK_a groups (like phenolic groups) were detected. It is suggested that most of the surface charge could therefore be attributed to other surface (aromatic) groups, such as those that are pyrone-like [36]. On the other hand, on CR_800Zn, there appear a considerable amount of slightly acidic groups of $pK_a < 7$, which is a natural feature of carbons that have been activated with ZnCl₂. Therefore, one can deduce that such carbons could be ideal for the removal of aromatic molecules with low polarity, in which π - π interactions dominate adsorption.

Figure 4A presents the XPS-survey spectra of the CR_600 sample, with peaks corresponding to C 1s, N 1s, O 1s, and Cr 2p and smaller peaks of Cl 2p and Si 2p. The high-resolution spectrum at the Cr 2p region was deconvoluted in two peaks at 576.2 eV and 585.5 eV, related with

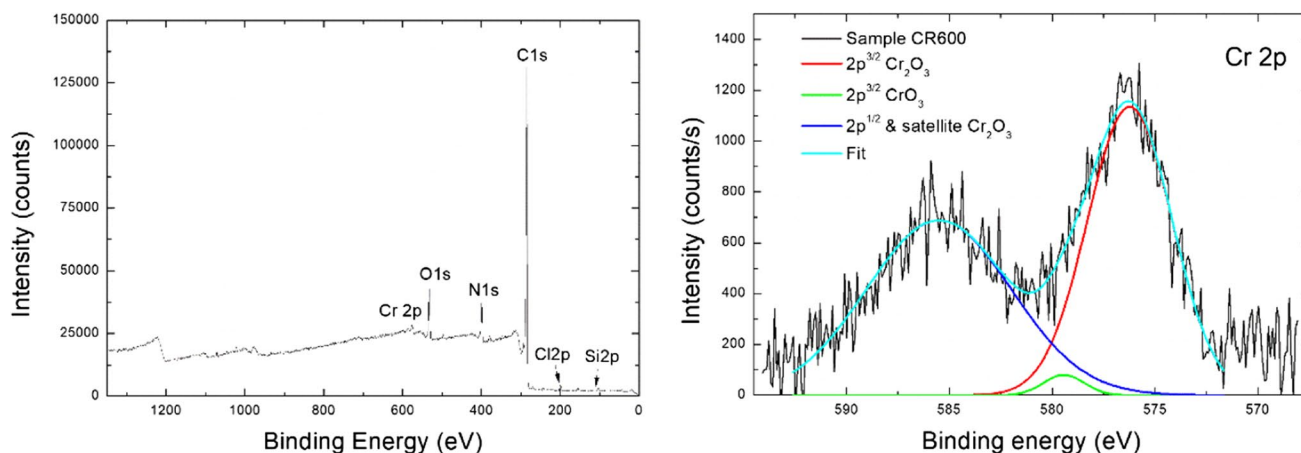


Fig. 4 **A** XPS survey spectrum and **B** high-resolution spectra at the Cr 2p range of the CR600 sample

Table 4 Textural properties of synthesized materials

Material	S_{BET} [m^2/g]	Vtot [cm^3/g]
CR_600	0	0
CR_800	1	0
CR_800Zn	585	0.237

Cr $2p^{3/2}$ and a Cr $2p^{1/2}$ satellite in Cr_2O_3 , and a small subtle peak at 579.4 eV, probably related with CrO_3 [37].

The images of the synthesized materials are displayed in Figure S4. The surface of the carbon materials is striated and apparently has a low pore content. A magnified image demonstrated that the surface is richly porous, particularly that of CR_800Zn, which is expected, due to the activating effect of ZnCl_2 .

Although some porosity was suggested in the SEM images, nitrogen physisorption isotherms of CR_800 and CR_800Zn (Fig. S5) demonstrated that the non-activated materials had a low surface area, which considerably improved upon ZnCl_2 addition. The surface area (Table 4) increased from $\sim 1 \text{ m}^2/\text{g}$ up to $585 \text{ m}^2/\text{g}$, which is a

considerable surface area, taking into consideration that the precursor was a non-lignocellulosic material.

3.3 Dye adsorption study using the carbons obtained from de-chromed tanned leather shavings

Adsorption experiments were carried out with the objective of removing pollutant dyes of different chemical configurations and sizes. The adsorption isotherms at pH 7 and 25°C are depicted in Fig. 5, and the fittings of the Langmuir and Freundlich isotherms are displayed in Table 5. Congo red adsorption capacity was better described by the Freundlich model, suggesting possible multilayer formation, as this adsorption is probably driven by π - π interactions between one or several of the aromatic rings on Congo red and the aromatic layers of the carbon benzene ring. On the contrary, methylene blue was better represented by the Langmuir model, as its adsorption is linked with pore availability and surface area.

On the adsorption isotherm of Congo red, it is interesting to note the lack of adsorption capacity of CR_600,

Fig. 5 Adsorption isotherms of **A** Congo red and **B** methylene blue on the synthesized materials

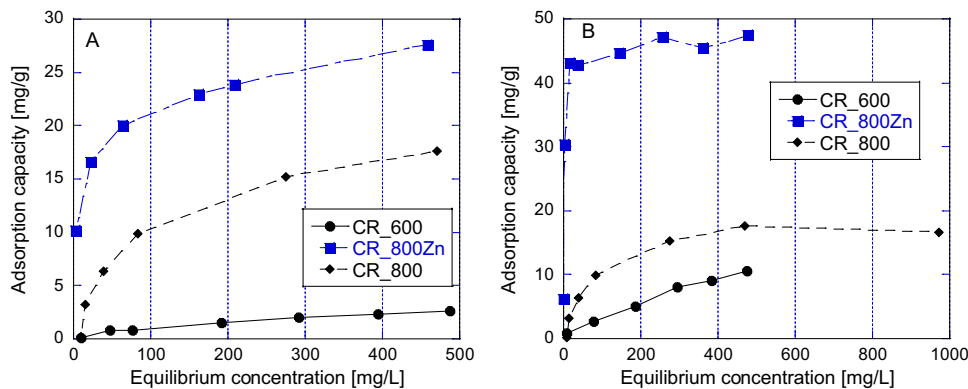


Table 5 Fittings of Langmuir and Freundlich models on the adsorption data

Material	Langmuir			Freundlich		
	Q^{max} [mg/g]	b [L/mg]	R^2	KF [(mg/g)(l/mg) ^{1/n}]	n	R^2
Congo red						
CR_600	4.082	0.003	0.9918	0.069	1.688	0.9934
CR_800	21.22	0.010	0.9936	0.010	21.22	0.9981
CR_800Zn	24.02	0.203	0.9064	8.892	5.244	0.9970
Methylene blue						
CR_600	27.370	0.001	0.9973	0.111	1.349	0.9968
CR_800	19.372	0.012	0.9902	1.803	2.879	0.9324
CR_800Zn	45.930	0.720	0.9977	23.832	8.092	0.8910

which remained below 5 mg/g, even at high concentrations. On the other hand, carbonization at 800 °C strongly improved the adsorption capacity up to 15 mg/g, and the activation process further improved adsorption up to greater than 25 mg/g. These are positive results, indicating that high carbonization temperatures of adsorbents are beneficial for the adsorption of dyes; however, such capacity is not entirely reflective of pore creation, since the surface area of CR_800 was still low compared with that of CR_800Zn. Therefore, the increase in adsorption capacity could be due to a combination of pore space for transport and a higher availability of aromatic rings in the carbonized material at the highest temperature. This feature has also been demonstrated in other biochars, in which materials synthesized at higher temperatures demonstrated a superior performance [38].

By contrast, methylene blue is a model dye, whose adsorption correlates very well with the available surface area [39]. As observed in the isotherms in Fig. 5, there is a relationship between capacity and S_{BET} ; therefore, the adsorption capacity of CR_800Zn was considerably higher than that of CR_800 and CR_600 (around 47 mg/g vs 17 mg/g and 10.5 mg/g, respectively at 470 mg/L). The adsorption results indicated that activation is an optional but helpful process to improve dye adsorption in Cr-free carbons. There is a considerable increase of adsorption capacity, but at a cost: the use of $ZnCl_2$ and water for the rinsing procedure. A comparison of the capacities recorded here with other materials available in the literature is presented (Table 6). These materials are comparable to other waste-derived biosorbents; however, note that they demonstrate a lesser capacity than other materials specifically designed to remove these dyes [40, 41].

Taking into consideration that Zn could be regenerated and employed for further use, and rinsing water can easily be treated, this process is excellent for obtaining a low inorganic content carbon for the removal of pollutants, such as dyes, from aqueous solution.

3.4 Characterization of the extraction liquor

The extraction liquor is rich in chromium (III) ions and also in hydrolyzed proteins and amino acids [54], and therefore can be employed as a re-tanning agent; hence, the liquor was characterized first. To determine the amino acid and protein contents, the liquor was subject to an acidic precipitation, and separated by centrifugation and filtration through a Millipore system with a 0.45 μm membrane. The analysis was carried out in 4 extraction solutions, using cysteine and tyrosine as model amino acids (see Table 7). The objective was to elucidate if any particular condition promoted a lower or higher degree of hydrolysis, in comparison to the condition that was pre-selected for the carbon materials (condition 2 in Table 7).

The Bradford method of analysis demonstrated a low quantity of hydrolyzed proteins, indicating that the process was successful in hydrolyzing mainly the Cr–O bond, or that the protein bonds were too strong to be hydrolyzed to the amino acid level. Condition 2 demonstrated a low amount of hydrolyzed protein, corroborating that this process was indeed efficient in hydrolyzing only the Cr–O bond. Other authors have reported a high recovery (80–90%) of collagen proteins by using alkaline hydrolysis [15], and up to 80% [55] with enzymatic hydrolysis; however, this comes at the cost of hydrolyzing the whole structure, which was contrary to the primary objective of maintaining the leather structure and using the leftover solution for leather re-tanning.

The results of the amino acid extraction indicated only small amounts of cysteine (Cys) and tyrosine (Tyr) in the extraction solution, with no particular relationship to the concentrations of NaOH and K-tar. The results postulated that extraction does not increase the amount of hydrolyzed protein; however, remaining amino acids could be helpful during processes of chromium re-tanning. Therefore, we corroborated that 0.17 NaOH and 1.5 M K-tar (condition 2) are the ideal extraction conditions to obtain both the activated carbons and the re-tanning solution.

Table 6 Comparison of the adsorption capacities of other materials available in the literature

Type of material	Adsorbate	Experimental conditions	Capacities reported	Reference
Chromium-tanned leather shavings	Methylene blue	30–100 mg/L pH uncontrolled 25 °C	ca 75 mg/g at 100 mg/L	[42]
Biochar from palm frond	Methylene blue	2–200 mg/L pH 2 25 °C	206 mg/g (Q_{max}) ca 160 mg/g at 100 mg/L	[43]
Sewage-derived biochar	Methylene blue	50–150 mg/L pH 6 25 °C	24.10 mg/g (Q_{max}) ca. 22.6 at 100 mg/L	[44]
Pine wood biochar	Methylene blue	0–500 mg/L	4 mg/g (Q_{max})	[45]
Pig manure biochar		pH 6.5	16.3 mg/g	
Paper-derived biochar		25 °C	1.6 mg/g	
Activated carbon from <i>Rosa canina</i> sp. seeds	Methylene blue	0–12 mg/L pH 6.5 20 °C	47.2 mg/g ca. 10 mg/g	[46]
Corn cob activated carbon	Methylene blue		0.84 mg/L N.M	[47]
Ashitaba wastes–activated carbon	Methylene blue Congo red	0–50 mg/L 25 °C pH 7 0–90 mg/L	~60 mg/g at 40 mg/L ~300 mg/g at 80 mg/L	[48]
Fly ash waste	Congo red	20 °C	22.12 mg/g (Q_{max})	[49]
Guava peel activated carbon	Congo red	30 °C pH 6	3.90 mg/g at 100 mg/L	[50]
Activated carbon prepared from <i>Martynia annua</i>	Congo red	pH 7.1	29.82 mg/g (Q_{max})	[51]
Activated carbon from <i>Myrtus communis</i>	Congo red	Room temperature pH 7	19.23 mg/g (Q_{max})	[52]
Carbons from leaves and stem of water hyacinth	Congo red	100–1000 mg/L 30 °C	13.44 mg/g (Q_{max})-stem 13.29 mg/g (Q_{max})-leaves	[53]
De-chrommed tanned leather shavings	Methylene blue Congo red	10–1000 mg/L 25 °C pH 7	45.30 mg/g at 470 mg/L 22.89 mg/g at 100 mg/L	This study

Table 7 Characterization of the extracted liquor

Condition No	NaOH [M]	K-tar [M]	Total protein [g/L]	Cys [mg/L]	Tyr [mg/L]	Chromium [mg/L]
1	0.05	0.5	0.031	0	28.8	332
2	0.17	1.5	0.005	3.3	697.8	467
3	0.1	2.5	0.070	1.3	1187.8	401
4	0.5	3.1	N.D	0	704.5	377

3.5 Use of extraction liquor as a re-tanning agent of wet blue leather

The procedure for re-tanning wet blue leather was described in Section 2.8. Due to the relatively high cost of potassium tartrate, a substitution with sodium formate was employed. The finished leather, re-tanned with extracted chromium-rich solution, was compared with a Cr33 re-tanned sample. The concentration of C_2O_3 in the formate extract was 37.84 g/L. The formula described in Table S3 takes into account the

amount of chromium in the extraction liquor so that both products could have the same chromium concentration on the tanned leather.

It was determined that both Cr33 and the liquor solution had a high absorption factor onto leather (higher than 99%). The images of the finished leather are provided in Figure S6; Table 8 displays the basic characterization of subjective and physical properties of the liquor re-tanned and Cr33 re-tanned materials. Both subjective and physical properties are determinant factors for addressing the quality of a

Table 8 Tanning results of leather re-tanned with chromium-rich liquor vs Cr33

Re-tanning	Softness	Tact	Filling	Color intensity	Grain tear (N/mm)	Tensile strength (MPa)	Elongation at break (%)	Tear (kg)
Liquor re-tanned	3	3	4	5	8	243	44	5.6
Cr33 re-tanned	3	4	5	4	7.8	176	40	3.8

finished leather. The former results from consumer evaluation of leather materials primarily by touch [56]. The latter is due to the importance of such features as resistance and strength, essential parameters that determine if the leather is suitable for a certain application (e.g., shoe making or upholstery). An evaluation of our re-tanned leather with the Cr33 finished leather allows for a direct comparison of both factors, and provides insight about the quality of leather.

The subjective properties of the finished leather were divided into 5 levels: 1. Very poor, 2. Poor, 3. Fair, 4. Good, and 5. Very good.

In terms of softness, tact, filling, and color intensity, the two leather materials performed similarly, with slightly better average scores for Cr33 re-tanned leather. However, in terms of physical resistance, the liquor re-tanned leather demonstrated a better performance, particularly in terms of tensile strength (38% higher). Such improvement is probably due to the presence of amino acids and hydrolyzed proteins that efficiently fill the leather therefore, improving the uptake of fats and stabilizing the collagen fibers. The obtained results, in terms of tensile strength and elongation at break, are similar to those reported for goatskin [57], sheep [58], and cow [59], and can be employed for applications such as shoe making.

The results demonstrated that the processed liquor has the potential to be employed as a re-tanning agent. This is due to its high chromium and protein content. The organic anions, such as tartrate or formate, aid in decreasing the available number of coordination sites, which in turn helps to maintain soluble Cr-complexes and enhance the penetration of chromium into the leather.

4 Conclusions

The present article proposes a novel methodology for the processing of chromium-tanned leather shavings (CTLS). The process includes a NaOH hydrolysis of CTLS, aided by K-tar to obtain de-chromed tanned leather shavings (DTLS) and a chromium-rich liquor.

The DTLS were successfully transformed into biochar and activated carbon at 600 and 800 °C. In order to promote wider pore development and therefore a higher adsorption, an activating agent is preferred. Maximum adsorption capacities of 27.58 and 47.60 mg/g for Congo red and methylene

blue, respectively, were obtained. Due to the low surface charge developed, it is proposed that such adsorption is due to π - π interactions between the aromatic rings of the carbon materials and those of the dyes. The chromium-rich solution was successfully employed as a re-tanning agent on a wet blue bovine leather. The results demonstrated similarities, and in some cases an enhancement, of the properties of finished leather over that re-tanned with Cr33. The proposed study represents an excellent alternative for the management of hazardous leather shavings, as it produces a biochar/activated carbon and a re-tanning chromium solution, which in turn assist in reducing water pollution. Before scaling up the proposed refining process, it is of interest to develop a pilot adsorption study regarding the removal of not only dyes, but other pollutants (including those found in the tannery wastewater), and to obtain engineering parameters that allow for scaling up. This is part of our future work.

Supplementary Information The online version contains supplementary material available at <https://doi.org/10.1007/s13399-023-04014-1>.

Acknowledgements The authors are grateful with Ernesto Ornelas and Catalina de la Rosa for their technical assistance at CIATEC. The assistance of national laboratories LINAN and LANBAMA as well as the help of Ana Iris Maldonado during the microscopy measurements and Elizabeth Isaacs for the physisorption of nitrogen is appreciated. XPS analysis was performed by Engineer Wilian Javier Cauch at the National Laboratory of Nano and Biomaterials at CINVESTAV-Merida, sponsored by the following projects: FOMIX-Yucatan, 2008-1081160 and CONACYT LA-2009-01-123913, 292692, 294643, 188345, and 204822. Ionic chromatography analysis was sponsored by CONACYT through the project 269990.

Author contribution JA Arcibar-Orozco was in charge of the experimentation and planning of the manuscript, wrote the majority, and thoroughly reviewed it, A. Saldaña-Robles performed the design experimental analysis and wrote the corresponding discussion, R. Rangel-Mendez was in charge of most of the material's characterization, Lilja Nielsen wrote part of the manuscript and edited thoroughly, H. Baltazar-Campos performed all of the extraction and adsorption experiments, A. Garduño-Cruces performed the chromatography analysis and characterization of the protein, V. Hernandez-López assisted in the experimentation related to the leather re-tanning, and F. Caballero-Briones performed the XPS analysis and discussion.

Funding This work was supported by the Ministry for Innovation of Guanajuato (Secretaría de Innovación del Estado de Guanajuato, SICES) through the SICES/058/2018 grant and CONACYT (Ciencia de Frontera CF-2019 1727999).

Data availability Data will be available upon request.

Declarations

Ethical approval Not applicable.

Conflict of interest The authors declare no competing interests.

References

- Pati A, Chaudhary R, Subramani S (2014) A review on management of chrome-tanned leather shavings: a holistic paradigm to combat the environmental issues. *Environ Sci Pollut R* 21:11266–11282. <https://doi.org/10.1007/s11356-014-3055-9>
- Kolomaznik K, Adamek M, Andel I, Uhlířova M (2008) Leather waste—potential threat to human health, and a new technology of its treatment. *J Hazard Mater* 160:514–520. <https://doi.org/10.1016/j.jhazmat.2008.03.070>
- Muralidharan V, Palanivel S, Balaraman M (2022) Turning problem into possibility: a comprehensive review on leather solid waste intra-valorization attempts for leather processing. *J Clean Prod* 133021. <https://doi.org/10.1016/j.jclepro.2022.133021>
- Appala VNSG, Pandhare NN, Bajpai S (2022) Biorefining of leather solid waste to harness energy and materials—a review. *Biomass Convers Biorefin.* 1–18. <https://doi.org/10.1007/s13399-022-02455-8>
- Long H, Huang X, Liao Y, Ding J (2021) Recovery of Cr(VI) from tannery sludge and chrome-tanned leather shavings by Na₂CO₃ segmented calcination. *J Environ Chem Eng* 9:105026. <https://doi.org/10.1016/j.jece.2021.105026>
- Rigueto CVT, Nazari MT, Rosseto M, Massuda LA, Alessandretti IP, Piccin JS, Dettmer A (2021) Emerging contaminants adsorption by beads from chromium (III) tanned leather waste recovered gelatin. *J Mol Liq* 330:115638. <https://doi.org/10.1016/j.molliq.2021.115638>
- Li C, Xue F, Ding E (2015) Preparation of polyacrylamide grafted collagen extracted from leather wastes and their application in kaolin flocculation. *J Appl Polym Sci* 132. <https://doi.org/10.1002/app.41556>
- Gao D, Guo S, Zhou Y, Lyu B, Ma J, Zhao P, Pan D, Chen S (2022) Hydrophobic, flexible electromagnetic interference shielding films derived from hydrolysate of waste leather scraps. *J Colloid Interface Sci* 613:396–405. <https://doi.org/10.1016/j.jcis.2022.01.043>
- Tang Y, Zhao J, Zhang Y, Zhou J, Shi B (2021) Conversion of tannery solid waste to an adsorbent for high-efficiency dye removal from tannery wastewater: a road to circular utilization. *Chemosphere* 263:127987. <https://doi.org/10.1016/j.chemosphere.2020.127987>
- Manera C, Tonello AP, Perondi D, Godinho M (2019) Adsorption of leather dyes on activated carbon from leather shaving wastes: kinetics, equilibrium and thermodynamics studies. *Environ Technol* 40:2756–2768. <https://doi.org/10.1080/09593330.2018.1452984>
- Rao JR, Thanikaivelan P, Sreeram KJ, Nair BU (2002) Green route for the utilization of chrome shavings (chromium-containing solid waste) in tanning industry. *Environ Sci Technol* 36:1372–1376. <https://doi.org/10.1021/es015635s>
- Senthil R, Hemalatha T, Kumar BS, Uma TS, Das BN, Sastry TP (2015) Recycling of finished leather wastes: a novel approach. *Clean Technol Environ Policy* 17:187–197. <https://doi.org/10.1007/s10098-014-0776-x>
- Malek A, Hachemi M, Didier V (2009) New approach of depollution of solid chromium leather waste by the use of organic chelates: economical and environmental impacts. *J Hazard Mater* 170:156–162. <https://doi.org/10.1016/j.jhazmat.2009.04.118>
- Ferreira MJ, Almeida MF, Pinho SC, Gomes JR, Rodrigues JL (2014) Alkaline hydrolysis of chromium tanned leather scrap fibers and anaerobic biodegradation of the products. *Waste Biomass Valor* 5:551–562. <https://doi.org/10.1007/s12649-013-9252-9>
- Wionczyk B, Apostoluk W, Charewicz WA, Adamski Z (2011) Recovery of chromium(III) from wastes of uncolored chromium leathers. Part II. Solvent extraction of chromium(III) from alkaline protein hydrolyzate. *Sep Purif Technol* 81:237–242. <https://doi.org/10.1016/j.seppur.2011.07.024>
- Beltrán-Prieto JC, Veloz-Rodríguez R, Pérez-Pérez MC, Navarrete-Bolaños JL, Vázquez-Nava E, Jiménez-Islas H, Botello-Álvarez JE (2012) Chromium recovery from solid leather waste by chemical treatment and optimisation by response surface methodology. *Chem Ecol* 28:89–102. <https://doi.org/10.1080/02757540.2011.628016>
- Malek A, Hachemi M (2008) Effect of the detoxification on the shrinkage temperature and pH of chromium leather waste, another promising way for the tannery pollution. *Am J Appl Sci* 5:1329–1335. <https://doi.org/10.3844/ajassp.2008.1329.1335>
- Yahya MA, Al-Qodah Z, ZanariahNgah CW (2015) Agricultural bio-waste materials as potential sustainable precursors used for activated carbon production: a review. *Renew Sust Energ Rev* 46:218–235. <https://doi.org/10.1016/j.rser.2015.02.051>
- Arcibar-Orozco JA, Barajas-Elias BS, Caballero-Briones F, Nielsen L, Rangel-Mendez JR (2019) Hybrid carbon nanochromium composites prepared from chrome-tanned leather shavings for dye adsorption. *Water, Air, Soil Pollut* 230:142. <https://doi.org/10.1007/s11270-019-4194-x>
- Arcibar-Orozco JA, Rangel-Mendez JR, Bandosz TJ (2013) Desulfurization of model diesel fuel on activated carbon modified with iron oxyhydroxide nanoparticles: effect of tert-butylbenzene and naphthalene concentrations. *Energy Fuels* 27:5380–5387. <https://doi.org/10.1021/ef400999g>
- Jagiello J (1994) Stable numerical solution of the adsorption integral equation using splines. *Langmuir* 10:2778–2785. <https://doi.org/10.1021/la00020a045>
- Hammond JBW, Kruger NJ (1988) The Bradford method for protein quantitation. In: Walker JM (ed) *New protein techniques*. Humana Press, Totowa, NJ, pp 25–32
- ISO, 2017. ISO 20137:2017(en) Leather — chemical tests — guidelines for testing critical chemicals in leather. <https://www.iso.org/obp/ui/#iso:std:iso:20137:ed-1:v1:en>. (Accessed 09/09/2022)
- Wionczyk B, Apostoluk W, Charewicz WA, Adamski Z (2011) Recovery of chromium(III) from wastes of uncolored chromium leathers. Part I. Kinetic studies on alkaline hydrolytic decomposition of the wastes. *Sep Purif Technol* 81:223–236. <https://doi.org/10.1016/j.seppur.2011.07.036>
- Ke L, Zhao K, Yan X, Cao X, Wu X, Zhang C, Luo T, Ding T, Yan N (2022) Facile mineralization and valorization of Cr-containing leather shavings for electrocatalytic H₂O₂ generation and organic pollutant removal. *Chem Eng J* 437:135036. <https://doi.org/10.1016/j.cej.2022.135036>
- Appala VNS, Gunasri P, Naresh N, Bajpai S (2022) Biorefining of leather solid waste to harness energy and materials—a review. *Biorefin.* In press, *Biomass Convers.* <https://doi.org/10.1007/s13399-022-02455-8>
- Gauza-Włodarczyk M, Kubisz L, Mielcarek S, Włodarczyk D (2017) Comparison of thermal properties of fish collagen and bovine collagen in the temperature range 298–670K. *Mater Sci Eng C* 80:468–471. <https://doi.org/10.1016/j.msec.2017.06.012>
- Yılmaz O, CemKantarlı I, Yuksel M, Sağlam M, Yanik J (2007) Conversion of leather wastes to useful products. *Resour Conserv Recycl* 49:436–448. <https://doi.org/10.1016/j.resconrec.2006.05.006>
- Oliveira LCA, Guerreiro MC, Gonçalves M, Oliveira DQL, Costa LCM (2008) Preparation of activated carbon from leather waste: a new material containing small particle of chromium oxide. *Mater Lett* 62:3710–3712. <https://doi.org/10.1016/j.matlet.2008.04.064>
- Kong J, Yue Q, Huang L, Gao Y, Sun Y, Gao B, Li Q, Wang Y (2013) Preparation, characterization and evaluation of adsorptive

- properties of leather waste based activated carbon via physical and chemical activation. *Chem Eng J* 221:62–71. <https://doi.org/10.1016/j.cej.2013.02.021>
31. Chaudhary R, Pati A (2017) Adsorption isotherm and kinetics of tannic acid on to carbonized chrome tanned leather solid waste. *J Soc Leath Tech Ch* 112:198–206
 32. Karmegam PM, Natarajan P, Somasundaram S (2023) Effect of activating agents on the photocatalytic activity of chromium oxide based porous carbon photocatalysts derived from chrome-tanned leather buffing dust waste for the degradation of 2-chlorophenol. *Chem Eng J* 451:138553. <https://doi.org/10.1016/j.cej.2022.138553>
 33. Li K, Liu Q, Cheng H, Hu M, Zhang S (2021) Classification and carbon structural transformation from anthracite to natural coaly graphite by XRD, Raman spectroscopy, and HRTEM. *Spectrochim Acta A* 249:119286. <https://doi.org/10.1016/j.saa.2020.119286>
 34. Manoj B, Kunjomana AG (2012) Study of stacking structure of amorphous carbon by X-ray diffraction technique. *Int J Electrochem Sci* 7:3127–3134
 35. Aguilera C, González JC, Borrás A, Margineda D, González JM, González-Elipe AR, Espinós JP (2013) Preparation and characterization of CrO₂ films by Low Pressure Chemical Vapor Deposition from CrO₃. *Thin Solid Films* 539:1–11. <https://doi.org/10.1016/j.tsf.2013.04.118>
 36. Fuente E, Menéndez JA, Suárez D, Montes-Morán MA (2003) Basic surface oxides on carbon materials: a global view. *Langmuir* 19:3505–3511. <https://doi.org/10.1021/la026778a>
 37. Laboratory, Measurement Services Division of the National Institute of Standards and Technology Material Measurement (2012) NIST, XPS database. <https://srdata.nist.gov/xps>. (Accessed 23/06/2022)
 38. Chen Y-d, Lin Y-C, Ho S-H, Zhou Y, Ren N-q (2018) Highly efficient adsorption of dyes by biochar derived from pigments-extracted macroalgae pyrolyzed at different temperature. *Bioresour Technol* 259:104–110. <https://doi.org/10.1016/j.biortech.2018.02.094>
 39. Raposo F, De La Rubia MA, Borja R (2009) Methylene blue number as useful indicator to evaluate the adsorptive capacity of granular activated carbon in batch mode: influence of adsorbate/adsorbent mass ratio and particle size. *J Hazard Mater* 165:291–299. <https://doi.org/10.1016/j.jhazmat.2008.09.106>
 40. Rafatullah M, Sulaiman O, Hashim R, Ahmad A (2010) Adsorption of methylene blue on low-cost adsorbents: a review. *J Hazard Mater* 177:70–80. <https://doi.org/10.1016/j.jhazmat.2009.12.047>
 41. Raval NP, Shah PU, Shah NK (2016) Adsorptive amputation of hazardous azo dye Congo red from wastewater: a critical review. *Environ Sci Pollut R* 23:14810–14853. <https://doi.org/10.1007/s11356-016-6970-0>
 42. Tahiri S, Messaoudi A, Albizane A, Azzi M, Bouhria M, Younsi SA, Bennazha J, Mabrouj J (2003) Removal of dyes from aqueous solutions by adsorption on chrome-tanned solid wastes generated in the leather industry. *Water Qual Res J* 38:393–411. <https://doi.org/10.2166/wqrj.2003.025>
 43. Zubair M, Mùazu ND, Jarrah N, Blaisi NI, Aziz HA, Al-Harathi MA (2020) Adsorption behavior and mechanism of methylene blue, crystal violet, eriochrome black T, and methyl orange dyes onto biochar-derived date palm fronds waste produced at different pyrolysis conditions. *Water, Air, Soil Pollut* 231:240. <https://doi.org/10.1007/s11270-020-04595-x>
 44. Fan S, Wang Yi, Wang Z, Tang J, Tang J, Li X (2017) Removal of methylene blue from aqueous solution by sewage sludge-derived biochar: adsorption kinetics, equilibrium, thermodynamics and mechanism. *J Environ Chem Eng* 5:601–611. <https://doi.org/10.1016/j.jece.2016.12.019>
 45. Lonappan L, Rouissi T, Das RK, Brar SK, Ramirez AA, Verma M, Surampalli RY, Valero JR (2016) Adsorption of methylene blue on biochar microparticles derived from different waste materials. *Waste Manage (Oxford)* 49:537–544. <https://doi.org/10.1016/j.wasman.2016.01.015>
 46. Gürses A, Doğar Ç, Karaca S, Acikyildiz M, Bayrak R (2006) Production of granular activated carbon from waste *Rosa canina* sp. seeds and its adsorption characteristics for dye. *J Hazard Mater* 131:254–259. <https://doi.org/10.1016/j.jhazmat.2005.09.014>
 47. Tseng R-L, Tseng S-K, Wu F-C (2006) Preparation of high surface area carbons from Corn cob with KOH etching plus CO₂ gasification for the adsorption of dyes and phenols from water. *Colloids Surf A* 279:69–78. <https://doi.org/10.1016/j.colsurfa.2005.12.042>
 48. Li Z, Hanafy H, Zhang L, Sellaoui L, Schadeck N, Matias O, Marcos LS, Seliem MK, Luiz Dotto G, Bonilla-Petriciolet A, Li Q (2020) Adsorption of congo red and methylene blue dyes on an ashitaba waste and a walnut shell-based activated carbon from aqueous solutions: experiments, characterization and physical interpretations. *Chem Eng J* 388:124263. <https://doi.org/10.1016/j.cej.2020.124263>
 49. Harja M, Buema G, Bucur D (2022) Recent advances in removal of Congo Red dye by adsorption using an industrial waste. *Sci Rep* 12:6087. <https://doi.org/10.1038/s41598-022-10093-3>
 50. Singh P, Raizada P, Pathania D, Sharma G, Sharma P (2013) Microwave induced KOH activation of guava peel carbon as an adsorbent for congo red dye removal from aqueous phase. *Indian J Chem Technol* 20:305–311
 51. Sivakumar V, Asaithambi M, Sivakumar P, Gopal N (2014) Removal of Congo red dye using an adsorbent prepared from *Martynia annua*. L seeds *Am Chem Sci J* 4:424–442. <https://doi.org/10.9734/ACSJ/2014/6680>
 52. Ghaedi M, Tavallali H, Sharifi M, Kokhdan SN, Asghari A (2012) Preparation of low cost activated carbon from *Myrtus communis* and pomegranate and their efficient application for removal of Congo red from aqueous solution. *Spectrochim Acta A* 86:107–114. <https://doi.org/10.1016/j.saa.2011.10.012>
 53. Extross A, Waknis A, Tagad C, Gedam VV, Pathak PD (2022) Adsorption of congo red using carbon from leaves and stem of water hyacinth: equilibrium, kinetics, thermodynamic studies. *Int J Environ Sci Technol*. <https://doi.org/10.1007/s13762-022-03938-x>
 54. Kanagaraj J, Chandra Babu NK, Mandal AB (2008) Recovery and reuse of chromium from chrome tanning waste water aiming towards zero discharge of pollution. *J Clean Prod* 16:1807–1813. <https://doi.org/10.1016/j.jclepro.2007.12.005>
 55. Pati A, Chaudhary R, Subramani S (2013) Biochemical method for extraction and reuse of protein and chromium from chrome leather shavings: a waste to wealth approach. *J Soc Leath Tech Ch* 108:365–372
 56. Kim W (2021) A study on the subjective feeling affecting tactile satisfaction of leather in automobile: a structural equation modeling approach. *Int J Ind Ergon* 84:103167. <https://doi.org/10.1016/j.ergon.2021.103167>
 57. Dayanandan A, Kanagaraj J, Sounderraj L, Govindaraju R, Rajkumar GS (2003) Application of an alkaline protease in leather processing: an ecofriendly approach. *J Clean Prod* 11:533–536. [https://doi.org/10.1016/S0959-6526\(02\)00056-2](https://doi.org/10.1016/S0959-6526(02)00056-2)
 58. Habib AB, Noor IA, Musa AE (2015) Effect of some skin defects on physical properties of the leather. *J Appl Ind Sci* 3:112–119
 59. Ali F, Kamal M, Shoriful IM (2020) Comparative study on physical properties of different types of leather in Bangladesh. *Int J Eng Res Appl* 10:55–63. <https://doi.org/10.9790/9622-1002035563>

Publisher's note Springer Nature remains neutral with regard to jurisdictional claims in published maps and institutional affiliations.

Springer Nature or its licensor (e.g. a society or other partner) holds exclusive rights to this article under a publishing agreement with the author(s) or other rightsholder(s); author self-archiving of the accepted manuscript version of this article is solely governed by the terms of such publishing agreement and applicable law.